

## ARTICLE

# Structured cyclic peptide mimics by chemical ligation

Bethany C. Atkinson  | Andrew R. Thomson 

School of Chemistry, University of Glasgow,  
Glasgow, UK

## Correspondence

Andrew R. Thomson, School of Chemistry,  
University of Glasgow, Glasgow G12 8QQ,  
UK.

Email: [drew.thomson@glasgow.ac.uk](mailto:drew.thomson@glasgow.ac.uk)

## Funding information

University of Glasgow

## Abstract

We report the development of a  $\beta$ -turn mimic that allows the direct formation of cyclic peptides through a spontaneous cyclisation under standard solid phase peptide synthesis (SPPS) cleavage conditions. The mimic is formed via an acylhydrazone, which is either reduced in situ by triisopropylsilane-trifluoroacetic acid, or which can be isolated and reduced in a separate step. This method uses commercially available reagents and is compatible with manual and automated SPPS methods. The cyclisation is tolerant of polar residues at the C-terminal position, with the exception of asparagine, for which a subsequent structural rearrangement similar to aspartimide formation was observed. The cyclisation method has been shown to tolerate ring sizes equivalent to 5–10 amino acid residues. We have used this method to design and synthesise potential selective integrin binding sequences with controlled conformations.

## KEYWORDS

$\beta$ -turn mimic, chemical ligation, cyclic peptide, molecular dynamics

## 1 | INTRODUCTION

The biological activity exhibited by peptides such as hormones and venoms<sup>[1–3]</sup> is a function of their three-dimensional structure. The ability to target a specific conformational state is an outstanding challenge in the design of small bioactive peptides.<sup>[4]</sup> The presence of cyclic constraints in peptide systems reduces the number of conformational states available, and can therefore be used as a strategy to predispose the molecule to a particular 3D shape. In a biological context this can confer desirable properties such as protease resistance and stronger binding.<sup>[5]</sup> As such, cyclic peptides hold a great deal of promise as biologically active molecules. However, the synthesis of cyclic peptides is not always straightforward, usually requiring the manipulation of additional protecting groups, or cyclisation through comparatively labile disulfide bonds.<sup>[6–10]</sup> Perhaps more significantly, simply cyclising a peptide does not necessarily restrict it to one specific conformation. Therefore, the design of cyclic peptides with a specific, targeted conformation is an outstanding challenge in *peptide science*. One strategy to address this is to include subsequences that favour turn formation, such as those containing proline and/or a D-amino acid residue. The inclusion of a single D-amino acid in a peptide generally leads to the formation of a type II'  $\beta$ -turn and has been shown to reduce

the conformational freedom when incorporated into cyclic peptides.<sup>[4]</sup> As such, the presence of ordered  $\beta$ -turns is associated with reduced conformational freedom in cyclic peptides.

We have recently developed a ligation junction that allows the facile connection of two peptide units under mild conditions, and in doing so generates a  $\beta$ -turn mimic that replicates the key  $i - i + 3$  hydrogen bond of a  $\beta$ -turn.<sup>[11]</sup> We have demonstrated that this mimic, referred to herein as *BTM*, is able to replace the  $i + 1$  and  $i + 2$  residues of a  $\beta$ -turn in a  $\beta$ -hairpin system (Scheme 1a), preserving the overall structure and stability of the hairpin. Here, we describe how this system has been extended to cyclisation reactions to produce structured cyclic peptide mimics (Scheme 1b).

## 2 | MATERIALS AND METHODS

### 2.1 | Safety information

All materials were handled in accordance with standard laboratory safety protocols. Eye protection, gloves and lab-coat were worn at all times. All chemical transformations were carried out in a fume hood.

This is an open access article under the terms of the [Creative Commons Attribution](https://creativecommons.org/licenses/by/4.0/) License, which permits use, distribution and reproduction in any medium, provided the original work is properly cited.

© 2022 The Authors. *Peptide Science* published by Wiley Periodicals LLC.

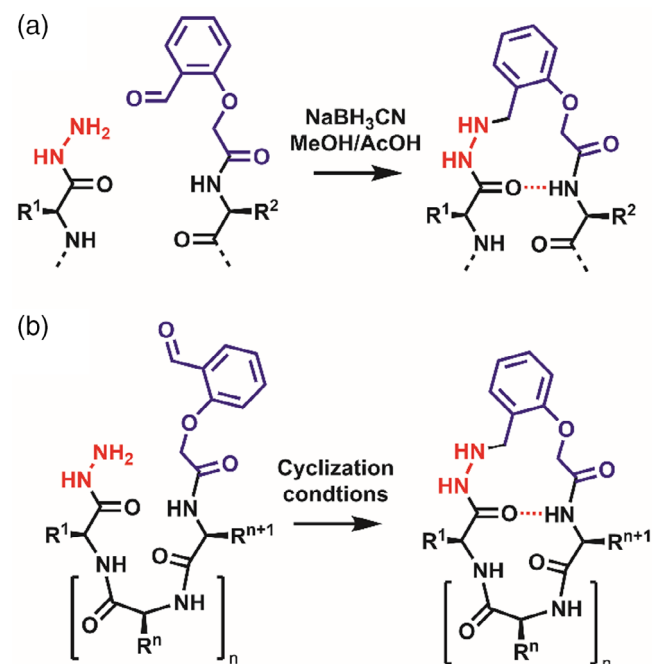
## 2.2 | General analytical procedures

High resolution mass spectrometry (HRMS) was performed on a Bruker microTOF-Q High Resolution Mass Spectrometer using ESI+ mode. Accurate mass data are detailed in Table S1.

Peptides were analysed on a Shimadzu reverse-phase HPLC system equipped with Shimadzu LC-20AT pumps, a Shimadzu SIL-20A autosampler and a Shimadzu SPD-20A UV-vis detector (monitoring at 214 and 280 nm) using a Phenomenex, Aeris, 5  $\mu$ m, peptide XB-C18, 150  $\times$  4.6 mm column at a flow rate of 1 ml/min. Gradients were run using a solvent system consisting of solution A (H<sub>2</sub>O + 0.1% TFA) and B (MeCN + 0.1% TFA). A gradient from 0% to 50% solution B over 30 min was used.

LC-MS analysis was performed on a Thermo Scientific LCQ Fleet quadrupole mass spectrometer using positive mode electrospray ionisation (ESI+). Gradients were run using a solvent system consisting of solution A (95/5 H<sub>2</sub>O/MeCN and 0.1% TFA) and B (95/5 MeCN/H<sub>2</sub>O and 0.1% TFA). The gradient used was linear, from 0% to 50% solution B over 10 min.

Peptides were purified on a reverse-phase Dionex HPLC system equipped with Dionex P680 pumps and a Dionex UVD170U UV-vis detector (monitoring at 214 nm and 280 nm), using a Phenomenex, Gemini, C18, 5  $\mu$ m, 250  $\times$  21.2 mm column at a flow rate of 8 ml/min. Gradients were run using a solvent system consisting of A (H<sub>2</sub>O + 0.1% TFA) and B (MeCN + 0.1% TFA). Collected fractions were lyophilised on a Christ Alpha 2-4 LO plus freeze dryer.



**SCHEME 1** Original  $\beta$ -turn mimic (a) and cyclisation (b)

## 2.3 | General procedure for peptide synthesis

### 2.3.1 | Synthesis of the hydrazine resin

Cl-trityl resin (0.25 g, 0.8 mmol/g) was pre-swelled in 1:1 DMF/CH<sub>2</sub>Cl<sub>2</sub>. Hydrazine hydrate (20 eq, ~80%) in DMF (6 ml) was added to the resin and left to react for 30 min. The resin was then washed four times with DMF and the reaction repeated. 10% methanol in DMF (6 ml) was added to the resin and left to react for 30 min to cap any remaining unreacted sites.

### 2.3.2 | Peptide synthesis

Peptides were synthesised using standard Fmoc/tBu solid phase peptide synthesis (SPPS) protocols on a 0.033 mmol scale on a CEM Liberty Blue peptide synthesis instrument. DIC/OxymaPure activation chemistry was used. The first residue of each sequence was double coupled to ensure efficient resin loading.

### 2.3.3 | Coupling of aldehyde

2-Formylphenoxy acetic acid (5 eq) was coupled using oxyma (4.5 eq), DIPEA (6 eq), DIC (4.5 eq) in 6 ml DMF for 2.5 h.

### 2.3.4 | Cleavage procedures

*Standard cleave:* 95% TFA, 2.5% water and 2.5% TIPS (5 ml total volume) was added to the resin and it was mixed gently for 2 h.

*Reductive cleave:* 90% TFA, 10% TIPS (5 ml total volume) was added to the resin and heated for 30 min at 50 °C or 2 h at room temperature with stirring.

*Cleave for the borohydride reduction:* 95% TFA, 5% water (5 ml total volume) was added to the resin and it was mixed gently for 2 h.

After cleavage the mixture was reduced in volume under a gentle flow of nitrogen gas followed by precipitation of the peptides in cold diethyl ether (40 ml). Precipitates were dissolved in 1:1 H<sub>2</sub>O/MeCN and lyophilised to yield white to off-white powders.

### 2.3.5 | Borohydride reduction

The peptide was dissolved in 1:1 MeOH:AcOH (5 ml total volume) and sodium cyanoborohydride (10 eq) was added and the mixture stirred for 15 min. The solvent was then evaporated and the product purified by preparative HPLC.

## 2.4 | Computational

Partial charges for the BTM unit were generated using antechamber with the bcc charge scheme. All models were built using Chimera,<sup>[12]</sup>

and then Bias-exchange metadynamics (BE-META) simulations were carried out using Gromacs 4<sup>[13]</sup> with the Plumed 2.5 plugin.<sup>[14]</sup> The peptides were immersed in a cubic box of explicit TIP3P water with a minimum of 1.0 nm between the peptide and the edge of the box. A steepest descent algorithm was then used followed by a four-stage equilibration process. First a 50 ps NVT ensemble was carried out followed by a 50 ps NPT ensemble both with 1000 kJ mol<sup>-1</sup> nm<sup>-2</sup> restraints on the heavy atoms. A 100 ps NVT ensemble followed by a 100 ps NPT ensemble was then carried out, this time without restraints. A separate V-rescale thermostat was used for both the peptide and the solvent to prevent the hot solvent, cold solute problem. A Berendsen barostat with an isothermal compressibility of  $4.5 \times 10^{-5}$  bar<sup>-1</sup> was used for the NPT ensembles and the MD simulations. The final trajectory file from the NPT 100 ps ensemble was used for the MD simulations.

The BE-META simulations were carried out with a replica for each residue biased along its  $\phi$  and  $\psi$  angles, and then a replica for each residue biased along its  $\phi$  dihedral and the  $\psi$  dihedral of the next residue along. Gaussian hills of height 0.1 kJ mol<sup>-1</sup> and width 0.3 radians were added every 4 ps. Additional unbiased replicas were also included. The BE-META simulations were carried out using a leapfrog algorithm with a timestep of 2 fs for 100 ns with exchanges attempted every 5 ps. An Amber99SB force field<sup>[15]</sup> was used and the simulations were carried out at 300 K and 1 bar. For the duration of the simulation all bonds to hydrogen atoms were constrained to equilibrium values using a LINCS algorithm. Non-bonded interactions (both Lennard-Jones and electrostatic) were truncated at 1 nm. For long range electrostatics a particle mesh Ewald (PME) with an order of four and Fourier spacing of 0.12 nm was used.

Backbone RMSD values were calculated using the align function in PyMOL.<sup>[16]</sup>

### 3 | RESULTS AND DISCUSSION

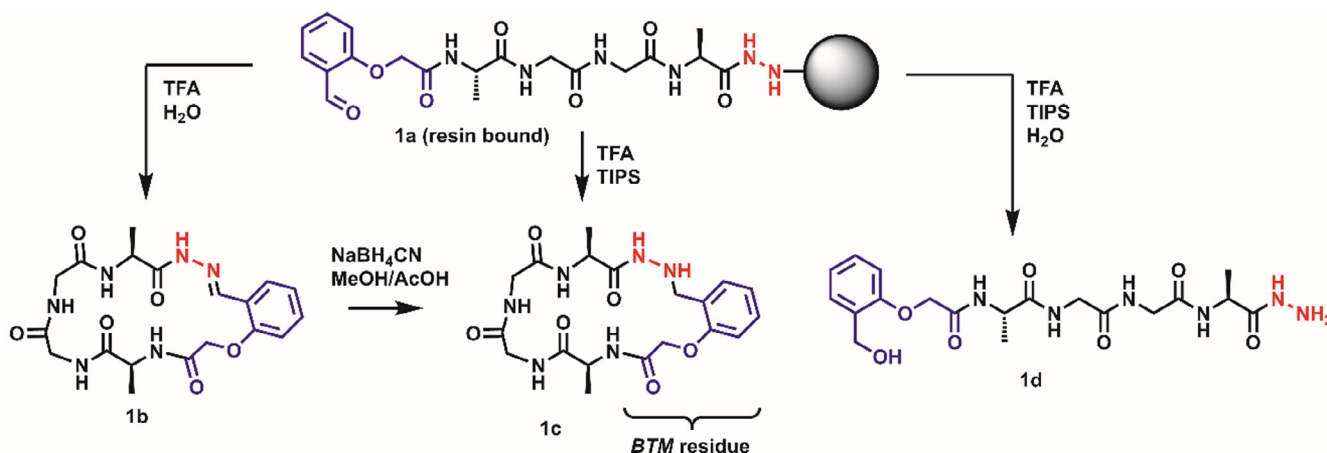
#### 3.1 | Cyclisation

We first established that our original  $\beta$ -turn mimic ligation junction was competent for the cyclisation of peptide substrates. Making use

of the AGGA subsequence as a model substrate we synthesised and purified peptide 1 (Scheme 2). This peptide was observed to exist in solution only as the cyclic acylhydrazone species, 1b, rather than the linear peptide 1a, suggesting that spontaneous cyclisation is favoured for rings of this size. The peptide was reduced to give the acylhydrazine linked species *cyclo*(BTM-AGGA), 1c, on treatment with sodium cyanoborohydride.

Furthermore, during the cleavage of peptide 1 from the solid support, we observed that the peptide cleavage cocktail of 2.5% triisopropylsilane (TIPS) and 2.5% water in trifluoroacetic acid (TFA) led to partial formation of 1c, as well as reduction of the aldehyde functionality of 1a to give the corresponding alcohol 1d. Based on this observation, as well as the poor compatibility of sodium cyanoborohydride in methanol/acetic acid mixtures with SPPS resins, we hypothesised that TFA/TIPS could form the basis of a mild reduction/cleavage protocol for the direct production of cyclic peptides, in which the acylhydrazone intermediate is formed and reduced in situ. Peptide 1 was therefore used as a model system to establish cyclisation conditions. We found that omission of water from the cleavage cocktail prevented the formation of the linear by-products and gave primarily the cyclic peptide as a mix of the acylhydrazone 1b and acylhydrazine 1c. Based on these findings we explored conditions for cyclative cleavage, and the results of this survey are summarised in Table 1. Our limited survey of cleavage conditions revealed that a relatively short cleave time of 30 minutes at an elevated temperature of 50 °C gave complete reduction of the acylhydrazone to the acylhydrazine.

Encouraged by these results, we tested the sequence tolerance of our cyclisation reaction using sequences 2–9 (Table 2, Scheme 3). In particular, we explored C-terminal residues with side chains that could present competing nucleophilic functionality or significant steric bulk. Because these are adjacent to the acylhydrazine group they have the potential to participate in competing reactions with the aldehyde group or otherwise affect its reactivity. With the exception of peptide 2, which contains the subsequence KPGN, all peptides yielded the desired cyclic structure. Peptide 6, containing a C-terminal Lys residue showed no evidence of competing reaction from the Lys side chain, in keeping with the higher nucleophilicity of the C-terminal acylhydrazine.



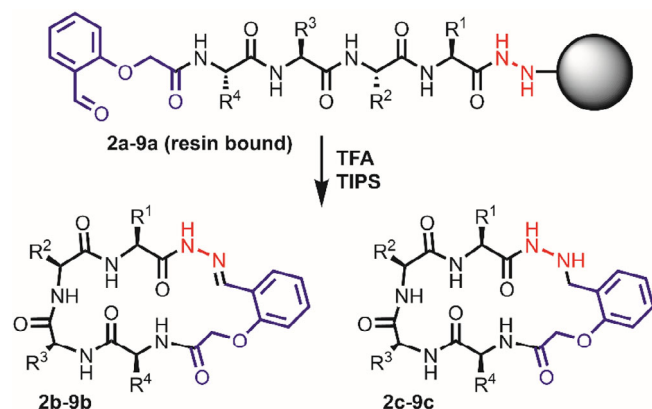
SCHEME 2 Synthesis of 1a–1d

**TABLE 1** Cleavage/cyclisation conditions and yields

Conditions	% TIPS in TFA	Temperature (°C)	Time (h)	% 1b reduced to 1c	Crude yield %
A	5	rt	0.5	64	57
B	10	rt	0.5	74	69
C	20	rt	0.5	64	60
D	10	rt	2	86	64
E	10	50	0.5	100	83

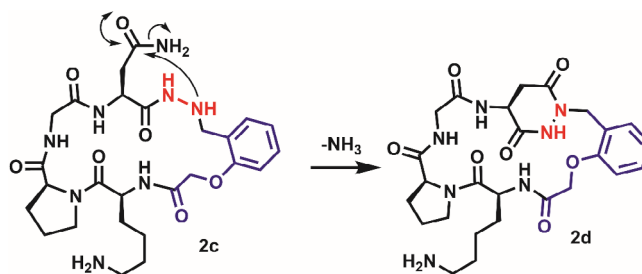
**TABLE 2** Sequences and yields for in situ cleavage/cyclisation of peptides 1–9

Peptide number	Peptide sequence	Crude yield (%)
1	c(BTM-AGGA)	83
2	c(BTM-KPGN) <sup>a</sup>	–
3	c(BTM-KPGD)	64
4	c(BTM-KPGQ)	81
5	c(BTM-KPGE)	77
6	c(BTM-QGPK)	77
7	c(BTM-KPGC)	7/63 <sup>b</sup>
8	c(BTM-KPGV)	83
9	c(BTM-KPGR)	84

<sup>a</sup>Side reaction observed.<sup>b</sup>Cleavage at room temperature.**SCHEME 3** Synthesis of peptides 2c–9c

Peptide 8, containing a C-terminal Val residue showed equal reactivity to peptide 1, which has a C-terminal Ala residue, indicating that steric hindrance from hydrophobic side chains is not a limiting factor. Given this finding, an exhaustive screen of hydrophobic residues was not carried out in this study. Under the cyclisation conditions employed only trace quantities of the acylhydrazone intermediates 2b–9b were detected.

In the case of peptide 2, KPGN, the peptide was observed to produce an alternative product with a mass 17 Da lower than that of the target compound. We posit that this is the cyclic acylhydrazone 2d, in analogy with aspartimide formation in peptide synthesis (Scheme 4).

**SCHEME 4** Proposed side reaction of peptide 2c

This product formed spontaneously over time from peptide 2c, indicating that it was not a consequence of the cleavage reaction conditions, but a fundamental reactivity of the peptide itself. A similar side reaction was not observed for the sequences 3, 4 or 5, containing C-terminal Asp, Gln and Glu residues, respectively, indicating that this is a specific property of the asparagine primary amide side chain. This is likely an inherent limitation of our  $\beta$ -turn mimic, arising from the nucleophilicity of the acylhydrazone.

The reductive cleavage of peptide 7, containing a C-terminal Cys residue, gave only modest yields (8%) of 7c under cleavage conditions E, presumably due to competing reactions involving the thiol side chain of the Cys residue. Lowering the temperature of this cleavage to room temperature (Table 1, conditions D), gave 7c in a 62% yield.

### 3.2 | Macrocycle ring size

We tested the ring size tolerance of our cyclisation protocol through the sequences shown in Table 3. In all subsequences except for PG the peptide cyclised through the  $\beta$ -turn mimic was observed. For sequence 10, PG, only the dimeric macrocycle *cyclo*-(BTM-PG)<sub>2</sub> was observed as product in a 38% yield, presumably due to the strained nature of the smaller ring. We observed a 38% yield of the cyclic product for peptide 11, KPG, but a 55% yield for peptide 12, KAG, indicating that the nature of the intervening peptide sequence can have a significant influence on cyclisation efficiency.

The larger peptides AKPGA, ASKPGA and SAKPGASA were also synthesised. Although the cyclic peptide was observed in each case, with increasing size the one-step cyclisation becomes increasingly inefficient, with numerous side products appearing. This is consistent with the formation of the intermediate acylhydrazone being less

favourable with increasing ring size. For comparison, SAKPGASA was synthesised using sodium cyanoborohydride as a reductant in a separate step after non-reductive cleavage from the resin which allows the hydrazone to form separately. For peptide 16, which is the equivalent of a cyclic decapeptide, a yield of 77% was seen using the two-step sodium cyanoborohydride method compared to a yield of 17% using the one-step conditions.

**TABLE 3** Variation of macrocycle ring size

Peptide number	Peptide sequence	Product (%)
10	c(BTM-PG)	0
11	c(BTM-KPG)	38
12	c(BTM-KAG)	55
13	c(BTM-APG)	55
14	c(BTM-AKPGA)	65
15	c(BTM-AKPGSA)	54
16	c(BTM-SAKPGASA)	17/77 <sup>a</sup>

<sup>a</sup>Yields for in situ and two-step cyclizations, respectively.

**TABLE 4** RGD-containing peptides

Peptide number	Peptide sequence	Product (%)
17	c(BTM-RGD)	77
18	c(BTM-SLSPGRGD)	34

### 3.3 | RGD peptides

In order to investigate the conformational influence of our cyclic BTM containing peptides on biologically relevant peptide sequences, we explored cyclic peptides containing the well-investigated integrin binding subsequence RGD.<sup>[17]</sup> To this end we designed two RGD-containing peptide sequences 17 and 18, Table 4. The smaller sequence, peptide 17 is intended to mimic cilengitide, a known agonist of the  $\alpha v \beta 3$  and  $\alpha v \beta 5$  integrins.<sup>[18,19]</sup> Peptide 18 was designed to mimic the extended linear conformation observed in crystal structures of native RGD containing ligands bound to  $\alpha IIb \beta 3$  integrins.<sup>[20]</sup> As such peptide 18 is designed to be a cyclic  $\beta$ -hairpin, with a PG turn sequence and  $\beta$ -strand favouring SLS sequence opposite the BTM unit and RGD subsequences, respectively. Peptides 17 and 18 were synthesised using our one-step cyclisation/cleavage protocol, in crude yields of 77% and 34%, respectively.

### 3.4 | Molecular dynamics simulations

In order to explore the conformational behaviour of these peptides we made use of BE-META molecular dynamics (MD) simulations, Figure 1. BE-META is an enhanced sampling technique that has been shown to be effective in predicting the conformation of cyclic peptides.<sup>[21,22]</sup> In each case we compared the results of our MD simulations with known 3D structures of the RGD peptide sequence bound

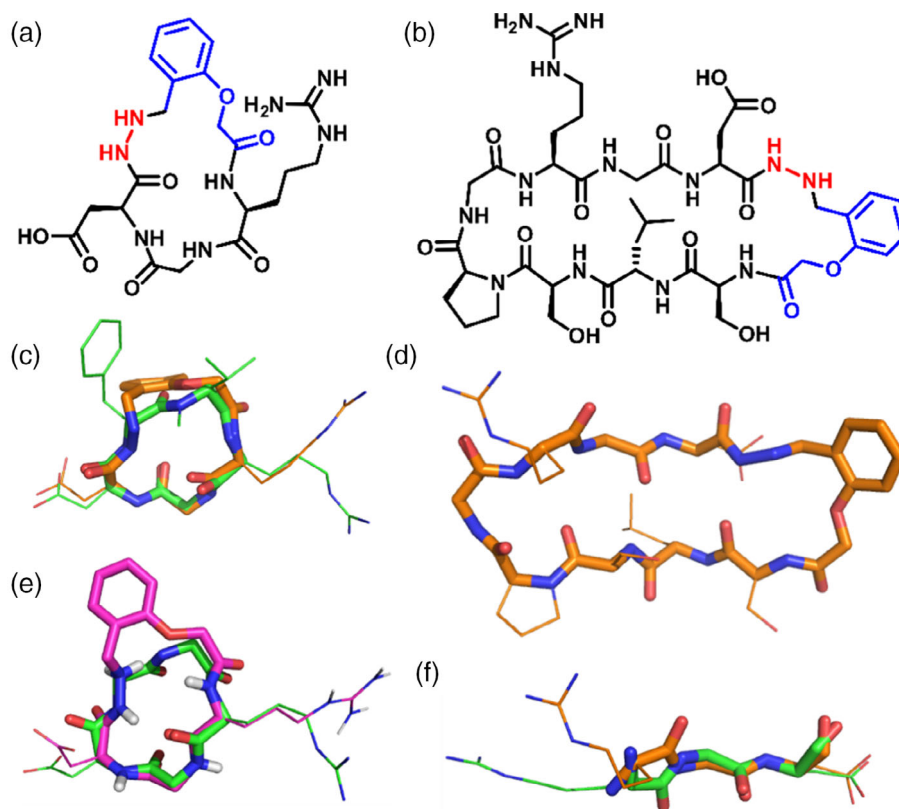


**FIGURE 1** (a) Structures of peptide 17. (b) Structure of peptide 18. (c) Overlay of major conformer of 17 (shown in orange) with cilengitide (green). (d) Major conformer of 18. (e) Overlay of minor conformer of 17 (magenta) with cilengitide (green). (f) Overlay of RGD subsequence of major conformer of 18 (orange) with RGD sequence of bound peptide (green)



to different integrin receptors. c(RGD-BTM) 17 was compared to the structure of cilengitide when bound to the extracellular segment of  $\alpha V\beta 3$  integrin (PDB: 1L5G). Peptide 18 was compared to the structure of the small peptide LGGAKQRGDV when bound to  $\alpha II\beta 3$  integrin (PDB: 2VDR).

Our simulations for peptide 17 reveal two major conformations in an approximate 2:1 ratio, Figure S1:. Both conformations are similar, differing only in at the aspartic acid residue, which appears in the  $\beta$ -sheet region of the Ramachandran plot for the major conformer, and the  $\alpha$  region for the minor one. In either case the similarity to the backbone region for the RGD subsequence in cilengitide is marked, with a backbone RMSD value of 0.201 Å for the major cluster and 0.281 Å for the minor. We therefore anticipate that this peptide will, like cilengitide, act as a binder of  $\alpha V\beta 3$  and  $\alpha V\beta 5$  integrins.

Our BE-META simulations indicate that peptide 18 adopts one major structure in which the central PG residues of the SLSPGRGD subsequence adopts a type II  $\beta$ -turn conformation, Figure S1:. The regions between this  $\beta$ -turn and the BTM  $\beta$ -turn mimic are held in a  $\beta$ -sheet structure. This results in the RGD motif adopting a linear conformation that closely approximates that of the bound RGD unit in the crystal structure of  $\alpha II\beta 3$  with a backbone RMSD of 0.903 Å. Taken together, these simulations indicate that the BTM unit, along with careful design of peptide sequence, can be used both as a means of cyclisation, and as a means of controlling peptide conformation.

In both peptide 17 and 18 the BTM unit acts as a turn, and facilitates the targeted geometry in the RGD subsequence. In each case, the BTM unit does not replicate a  $\beta$ -turn like hydrogen bond as previously observed in less constrained  $\beta$ -hairpin systems.<sup>[11]</sup> This suggests that the BTM unit is flexible enough to allow cyclic peptide formation, without the imposition of excessive steric constraints on the macrocycle.

## 4 | CONCLUSIONS

In conclusion, we have shown that the  $\beta$ -turn mimic BTM can be used as a means of producing cyclic peptide structures directly from the cleavage reaction following SPPS. Cyclic peptide mimics of sizes equivalent to 5–10 residues can be produced in high yield, and only an asparagine residue was found not to be tolerated adjacent to the ligation junction. For smaller ring sizes, up to an equivalent of seven residues, a one-step cleavage-cyclisation protocol was effective. For larger ring sizes a two-step protocol of peptide cleavage followed by separate reduction of the acylhydrazone proved to give the cyclic peptide in higher yield. Our MD simulations show that our ligation junction acts not only as a covalent connection, but also as a structure inducing element, giving rise to cyclic peptide mimics that have a well-defined conformation.

## ACKNOWLEDGMENTS

We thank University of Glasgow for funding.

## CONFLICT OF INTEREST

There are no conflicts of interest.

## DATA AVAILABILITY STATEMENT

Peptide characterisation and details of the MD studies are available in the supporting information of this article.

## ORCID

Bethany C. Atkinson  <https://orcid.org/0000-0002-0955-2683>

Andrew R. Thomson  <https://orcid.org/0000-0002-1066-1369>

## REFERENCES

- [1] Y. Hamada, T. Shioiri, *Chem. Rev.* **2005**, *105*, 4441.
- [2] N.-H. Tan, J. Zhou, *Chem. Rev.* **2006**, *106*, 840.
- [3] A. A. Vinogradov, Y. Yin, H. Suga, *J. Am. Chem. Soc.* **2019**, *141*, 4167.
- [4] R. Jwad, D. Weissberger, L. Hunter, *Chem. Rev.* **2020**, *120*, 9743.
- [5] A. Zorzi, K. Deyle, C. Heinis, *Curr. Opin. Chem. Biol.* **2017**, *38*, 24.
- [6] C. Bechtler, C. Lamers, *RSC Med. Chem.* **2021**, *12*, 1325.
- [7] H. C. Hayes, L. Y. P. Luk, Y.-H. Tsai, *Org. Biomol. Chem.* **2021**, *19*, 3983.
- [8] R. Vanjari, E. Eid, G. B. Vamiseti, S. Mandal, A. Brik, *ACS Cent. Sci.* **2021**, *7*, 2021.
- [9] T. R. Oppewal, I. D. Jansen, J. Hekelaar, C. Mayer, *J. Am. Chem. Soc.* **2022**, *144*, 3644.
- [10] F. Wuest, M. Berndt, R. Bergmann, J. van den Hoff, J. Pietzsch, *Bioconjugate Chem.* **2008**, *19*, 1202.
- [11] S. Crecente-Garcia, A. Neckebroek, J. S. Clark, B. O. Smith, A. R. Thomson, *Org. Lett.* **2020**, *22*, 4424.
- [12] E. F. Pettersen, T. D. Goddard, C. C. Huang, G. S. Couch, D. M. Greenblatt, E. C. Meng, T. E. Ferrin, *J. Comput. Chem.* **2004**, *25*, 1605.
- [13] B. Hess, C. Kutzner, D. van der Spoel, E. Lindahl, *J. Chem. Theory Comput.* **2008**, *4*, 435.
- [14] The PLUMED consortium, *Nat. Methods* **2019**, *16*, 670.
- [15] C. Tian, K. Kasavajhala, K. A. A. Belfon, L. Raguette, H. Huang, A. N. Miguez, J. Bickel, Y. Wang, J. Pincay, Q. Wu, C. Simmerling, *J. Chem. Theory Comput.* **2020**, *16*, 528.
- [16] Schrödinger, LLC, *The PyMOL Molecular Graphics System, Version 1.8*, Schrödinger, LLC, New York **2015**.
- [17] T. G. Kapp, F. Rechenmacher, S. Neubauer, O. V. Maltsev, E. A. Cavalcanti-Adam, R. Zarka, U. Reuning, J. Notni, H.-J. Wester, C. Mas-Moruno, J. Spatz, B. Geiger, H. Kessler, *Sci. Rep.* **2017**, *7*, 39805.
- [18] R. Stupp, M. E. Hegi, T. Gorlia, S. C. Erridge, J. Perry, Y.-K. Hong, K. D. Aldape, B. Lhermitte, T. Pietsch, D. Grujicic, J. P. Steinbach, W. Wick, R. Tarnawski, D.-H. Nam, P. Hau, A. Weyerbrock, M. J. B. Taphoorn, C.-C. Shen, N. Rao, L. Thurzo, U. Herrlinger, T. Gupta, R.-D. Kortmann, K. Adamska, C. McBain, A. A. Brandes, J. C. Tonn, O. Schnell, T. Wiegel, C.-Y. Kim, L. B. Nabors, D. A. Reardon, M. J. van den Bent, C. Hicking, A. Markivskyy, M. Picard, M. Weller, *Lancet Oncol.* **2014**, *15*, 1100.
- [19] J.-P. Xiong, T. Stehle, R. Zhang, A. Joachimiak, M. Frech, S. L. Goodman, M. A. Arnaout, *Science* **2002**, *296*, 151.
- [20] T. A. Springer, J. Zhu, T. Xiao, *J. Cell Biol.* **2008**, *182*, 791.
- [21] S. M. McHugh, J. R. Rogers, S. A. Solomon, H. Yu, Y.-S. Lin, *Curr. Opin. Chem. Biol.* **2016**, *34*, 95.
- [22] S. M. McHugh, H. Yu, D. P. Slough, Y.-S. Lin, *Phys. Chem. Chem. Phys.* **2017**, *19*, 3315.

## SUPPORTING INFORMATION

Additional supporting information may be found in the online version of the article at the publisher's website.

**How to cite this article:** B. C. Atkinson, A. R. Thomson, *Pept. Sci.* **2022**, *114*(5), e24266. <https://doi.org/10.1002/pep2.24266>